

QBO generated inter-annual variations of the diurnal tide in the mesosphere

Hans G. Mayr¹, and John G. Mengel²

¹ Goddard Space Flight Center, Greenbelt, MD

² Science Systems & Applications, Inc., Lanham, MD

Prepared for Submission
to
Journal of Geophysical Research
May, 2004

Abstract: We report results from a study with the Numerical Spectral Model (NSM), which produces in the mesosphere significant inter-annual variations in the diurnal tide. Applying Hines' Doppler Spread Parameterization (DPS), small-scale gravity waves (GW) drive the Quasi-biennial Oscillation (QBO) and Semi-annual Oscillation (SAO). With a GW source that peaks at the equator and is taken to be isotropic and independent of season, the NSM generates near the equator a QBO with variable periods around 27 months and zonal wind amplitudes close to 20 m/s at 30 km. As reported earlier, the NSM reproduces the observed equinoctial maxima in the diurnal tide at altitudes around 95 km. In the present paper it is shown that the QBO modulates the tide such that the seasonal amplitude maxima can vary from one year to another by as much as 30%. Since the period of the QBO is variable, its phase relative to the seasonal cycle changes. The magnitude of the QBO modulation of the tide thus varies considerably as our long-term model simulation shows. To shed light on the underlying mechanism, the relative importance of the linearized advection terms are discussed that involve the meridional and vertical winds of the diurnal tide.

I. Introduction

Measurements from the ground (e.g., Avery et al., 1989; Manson et al., 1989) and with the UARS spacecraft (e.g., Hays et al., 1994; McLandress et al., 1996) have shown that the diurnal tide in the upper mesosphere exhibits large seasonal variations. The amplitude of the tide exhibits maxima during equinox, which have been attributed to variations in eddy viscosity (e.g., Geller et al., 1997; Yudin et al., 1997; Akmaev, 2001a). In the Numerical Spectral Model (NSM) discussed here, the seasonal variations were attributed in part also to the momentum deposition from small-scale gravity waves (Mayr et al., 1998, 2001a).

The diurnal tide is also observed to exhibit inter-annual variations (Burrage et al., 1995; Vincent et al., 1998; Lieberman, 1997). Hagan et al. (1999a) demonstrated with the linear GSWM model that the seasonal variations of the tide are affected significantly by the linearized advection terms associated with the background zonal winds. In a separate paper, however, Hagan et al. (1999b) was unable to show that the inter-annual variations could be attributed to the observed Quasi-biennial Oscillation (QBO).

Applying the Canadian Middle Atmosphere Model (CMAM), McLandress (2002) was able to generate with the QBO significant inter-annual variations in the tide. In this study, the upper

boundary of the model was at 98 km, and an 18-months QBO was generated with parameterized small-scale gravity waves (Hines, 1997) that produced zonal wind amplitudes exceeding 40 m/s at 30 km. To provide understanding, McLandress (2002) performed a diagnostic analysis with a linear model to demonstrate that the QBO effect on the tide could be attributed to the advection term associated with the meridional gradient of the mean zonal circulation.

It is the purpose of this paper to report on a study with the NSM, which produces inter-annual variations in the diurnal tide that are clearly generated by the QBO. Although our model is significantly different from that discussed by McLandress (2002), we basically confirm his finding.

II. Numerical Spectral Model

The Numerical Spectral Model (NSM) extends from the Earth's surface into the thermosphere, and its design and applications have been discussed in the literature (e.g., Chan et al., 1994; Mengel, et al., 1995; Mayr et al., 1997, 1998, 2001). For the zonal mean ($m = 0$), the model is driven by solar heating due to ultraviolet radiation in the mesosphere and stratosphere taken from Strobel (1978), and by extreme ultraviolet radiation in the thermosphere. The radiative loss is described in terms of Newtonian cooling adopted from Zhu (1989). The tides are driven exclusively by the migrating thermal excitation sources in the troposphere and stratosphere (Forbes and Garret, 1978). Non-migrating tides driven by convection or topographic forcing are not accounted for. The planetary waves are generated only through instabilities that arise in the mean zonal ($m = 0$) temperature and wind fields; i.e., no planetary wave source of any kind is prescribed in the model.

An integral part of the NSM is that it incorporates the Doppler Spread Parameterization (DSP) for small-scale gravity waves (GWs) developed by Hines (1997a, b). The DSP deals with a spectrum of waves interacting with each other to produce Doppler spreading, which in turn affects the interaction of the waves with the background flow. This GW parameterization has also been applied successfully in a variety of other global-scale models (e.g., Akmaev, 2001b; Mancini et al., 1997) and has been discussed extensively in the literature.

In the 3D version of the NSM discussed here, tropospheric heating is applied for the zonal mean ($m = 0$) to reproduce qualitatively the observed zonal jets near the tropopause and the accompanying latitudinal temperature variations. We earlier applied such a source in our 2D

version of the NSM to study its affect on the equatorial oscillations (QBO, SAO). This additional heat source also generates planetary waves through the instabilities that arise.

In the present version of the NSM, the upper boundary is at about 130 km, which is well above the region of primary interest. To account properly for the non-linear GW momentum source that drives the QBO in the model, the vertical step size is taken to be about 0.5 km below 120 km, which is much shorter than that applied in GCMs. The NSM is truncated, however, at the zonal and meridional wave-numbers $m = 4$ and $n = 12$ respectively.

III. Model Results

IIIa. The QBO Signature in the Tide

To reveal the inter-annual variations of the tide, we ran the NSM for more than 25 years. The results will show that the spectral features of the QBO are clearly present in the tide. Apparently depending on the phase and period of the QBO relative to the seasonal cycle, however, its signature in the tide varies considerably.

For a latitude near the equator and altitudes between 10 and 100 km, we present in Figure 1 the computed zonal winds averaged over 28 days, which show the equatorial oscillations generated in the model. During this time span from 2 to 8 years, the period of the QBO is close to 24 months, and the amplitude around 30 km is about 20 m/s, which is in qualitative agreement with observations. At higher altitudes around 65 km, the semi-annual oscillation (SAO) dominates with wind amplitudes close to 40 m/s.

For the same time span, we show in Figure 2 the computed amplitudes of the diurnal tide at 18°N and 4°N (Gaussian points). A running window of 28 days is applied, and the results are presented at 95 km where the UARS data were taken (Burrage et al., 1995). In Figures 2a and 2b, respectively, the meridional and zonal winds are presented. Considering that the QBO is a low-latitude phenomenon, we present in Figure 2c the computed zonal wind amplitudes at 4°N together with the histogram for the spectral content of the tide at this latitude.

In agreement with observations, the computed tides in Figure 2 reveal the characteristic amplitude maxima near equinox that have been discussed before. For the purpose of this paper, the inter-annual variations are of interest, and they are clearly evident. In Figures 2a and 2b, the amplitudes around the years 3, 5 and 7 are significantly smaller when compared with the years 4 and 6, which reveals the 2-year periodicity of the QBO. This periodicity is also apparent in the

zonal winds near the equator (Figure 2c), and the associated histogram has a peak near 25 months.

To show more clearly the QBO signature in the tide, we present in Figure 3 time altitude contour plots for the relative amplitude variations of the zonal winds. A running window of 182 days (1/2 year) is applied, and the amplitudes at a given altitude are normalized relative to the time average. While preserving and revealing the relative seasonal and inter-annual variations throughout the middle atmosphere, the exponential growth of the tide with altitude is thus effectively eliminated. As Figure 3a shows, the QBO signature in the tide at 18°N is pronounced below 50 km and it is well correlated with the zonal winds in Figure 2. Westward (negative) and eastward (positive) directed zonal winds cause the amplitude of the tide to decrease and increase respectively. Above 50 km, the QBO signature at 18°N is also apparent but the pattern is more complicated.

While the QBO periodicity is clearly seen at altitudes around 50 km and above 80 km, the signature is not well defined in the altitude range between 60 and 80 km. In this altitude range, the pattern is much clearer at low latitudes (Figure 3b). Apparently, the QBO joins the semiannual oscillation (SAO), with eastward and westward zonal winds during equinox and solstice respectively. Through the SAO, the QBO signature in the tide then extends into the upper mesosphere. At both latitudes, the amplitude variations of the tide reverse above 80 km. QBO and SAO related enhancements in the tide around equinox below 80 km lead to maxima around solstice above that altitude. This pattern is pronounced in the tide near the equator, but it is also evident at 18°N . At altitudes below 50 km and at low latitudes in particular (Figure 3b), the QBO related variations in the tide are not aligned or correlated with the zonal winds shown in Figure 1.

The complicated patterns in the tide revealed in Figure 2 are likely caused by the interplay between the advection terms that couple the tide to the mean zonal circulation. Among the advection terms, all of which are fully accounted for in the NSM, two are primarily important at low latitudes where the tide is large. The first one involves the latitudinal gradient of the zonal winds multiplied with the meridional winds of the tide, and its importance for the QBO signature was emphasized by McLandress (2002). The second one involves the vertical gradient of the zonal winds multiplied with the vertical winds of the tide, and this one peaks at the equator (unlike the first one that vanishes there).

With the $m = 0$ zonal winds, U , and the meridional and vertical winds of the tide, ΔV and ΔW respectively, the above defined advection terms are written in the form

$$\frac{1}{r} \frac{\partial U}{\partial \theta} \Delta V \equiv \frac{2\pi}{\lambda_{U\theta}} U \Delta V \quad (1)$$

$$\frac{\partial U}{\partial z} \Delta W \equiv \frac{2\pi}{\lambda_{Uz}} U \Delta W \quad (2)$$

where wavelengths, λ , are introduced for the meridional and vertical scale-length of the zonal winds. Considering the continuity equation for the tide, with similar notations,

$$\frac{1}{r} \frac{\partial \Delta V}{\partial \theta} \equiv \frac{2\pi}{\lambda_{\Delta V\theta}} \Delta V \approx \frac{\partial \Delta W}{\partial z} \equiv \frac{2\pi}{\lambda_{\Delta Wz}} \Delta W; \quad \frac{2\pi}{\lambda_{\Delta V\theta}} \Delta V \approx \frac{2\pi}{\lambda_{\Delta Wz}} \Delta W; \quad \frac{\lambda_{\Delta Wz}}{\lambda_{\Delta V\theta}} \Delta V \approx \Delta W \quad (3)$$

and substituting Eq. (3) into the term (2) then yields

$$\frac{\partial U}{\partial z} \Delta W \equiv \frac{2\pi}{\lambda_{Uz}} U \Delta W \approx \frac{2\pi}{\lambda_{Uz}} \frac{\lambda_{\Delta Wz}}{\lambda_{\Delta V\theta}} U \Delta V$$

to permit a comparison between the terms (1) and (2):

$$\frac{2\pi}{\lambda_{U\theta}} U \Delta V : \frac{2\pi}{\lambda_{Uz}} \frac{\lambda_{\Delta Wz}}{\lambda_{\Delta V\theta}} U \Delta V$$

Since $\lambda_{Uz} \approx \lambda_{\Delta Wz}$ and $\lambda_{U\theta} \approx \lambda_{\Delta V\theta}$, the two terms are of comparable magnitude. The first would tend to vanish at the equator, the second to peak there.

This is borne out by the numerical results shown in Figure 4, where we present contour plots of the computed accelerations. In (a) the term (1) is presented at 18° N, and in (b) the term (2) at 4° N near the equator. To reveal the QBO signature, the temporal variations were essentially removed from the tide with a running mean of about 5 years, and for the mean zonal winds ($m = 0$) a running mean of 1 year was taken. The QBO signature is clearly evident in both terms and at both latitudes. Below 60 km, the QBO is stronger at the equator. But at 18° N, the QBO signature is evident, and stronger, at all altitudes above 70 km.

IIIb. QBO and Intermittence of Tidal Variability

The QBO period in our model is highly variable, and we believe that the non-linear interaction with the SAO is in part the cause (Mayr et al., 1998). In Figure 5a we present the spectrum for the zonal winds at 4° N obtained from a computer run covering 26 years. This shows that the largest amplitudes occur at a period around 24 months. But a secondary maximum also occurs at around 28 months, and a still smaller one occurs near 35 months. These

periodicities also appear in the diurnal tide as shown in Figures 5b and 5c, which present the histograms for the zonal and meridional wind amplitudes at 4°N and 18°N respectively. Relative to the annual and semiannual amplitudes, the QBO related signatures in the spectra are much larger near the equator than at 18°N .

While Figure 5 clearly demonstrates the QBO signature in the tide statistically, the magnitude of the signature in our model varies considerably as is shown with Figure 6. In the top panel, we present with Figure 6a the zonal winds that describe the equatorial oscillations, the QBO and the SAO. The winds represent 182-day averages with the time independent component removed. In the lower two panels, the 182-day average of the tidal amplitude for the zonal wind at 4°N is presented along with the histogram. During the first 7 years, pronounced inter-annual variations are evident with periods close to 2 years. Vertical dashed lines connect the amplitude minima with positive zonal wind patches in the mesosphere that vary with the period of the QBO. After 7 years, however, the inter-annual variation of the tide virtually disappears, and the same is true for the zonal wind features above 50 km.

It is reasonable to expect that the magnitude of the inter-annual variation of the tide be affected by the period of the QBO and its phase relative to the seasonal cycle. When the eastward winds in the QBO reach their largest magnitude during a 6-month period between spring and fall equinox, for example, the SAO and QBO would reinforce each other. Under this condition, the QBO effect on the tide would be different (presumably larger) from what it would be if such an alignment did not occur. Given that the QBO period is variable and generally not synchronized by the seasonal cycle, the variability shown in Figure 6 is thus understandable.

Our numerical results show that the magnitude of the QBO effect on the tide not only is highly variable, it also reveals an intermittent pattern. In Figure 7 we present the zonal winds that describe the QBO at 30 km (a) along with the amplitudes of the diurnal tide for a running window of $\frac{1}{2}$ year. The zonal winds of the QBO vary between 15 and 25 m/s, and the period is typically around 24 months but can be as large as 36 months. The tide at 30 km (Figure 7b), small in magnitude, clearly reveals the QBO signatures that appear with almost constant phase shift. The tide at 95 km, in contrast, shows the QBO signature intermittently. In the zonal winds near the equator (Figure 7c), the QBO signature appears during the first 7 years, then disappears essentially for 10 years, appears again for 3 cycles, and then disappears again. A similar pattern is also evident in the meridional winds of the diurnal tide at 18°N shown in Figure 7d.

IV. Discussion and Summary

We have applied the Numerical Spectral Model (NSM) to simulate the inter-annual variations in the diurnal tide that have been observed with satellite measurement and ground-based observations. In the study presented here, the NSM produces a realistic QBO with amplitudes close to 20 m/s at 30 km and periods between 24 and 28 months (Figure 1).

Propagating upward from the source regions in the troposphere and stratosphere, the amplitude of the diurnal tide grows with altitude to reach peak values around 90 km. At these altitudes in the upper mesosphere, the QBO signature is clearly seen in the inter-annual or year-to-year variations shown in Figure 2. It is also seen in the spectral features from a computer run covering more than 25 years, which reveal pronounced correlations between the mean zonal winds ($m = 0$) and the tide (Figure 5).

Since the diurnal tide represents a vertically propagating wave, variations imposed at lower altitudes translate into variations higher up. With the QBO originating in the lower stratosphere, its effect thus may come into play at all altitudes throughout the middle atmosphere as the relative variations of the diurnal tide indicate that are shown in Figure 3. The QBO signature is clearly seen not only in the upper mesosphere but in the lower stratosphere as well. And the signature is seen at 18°N (Figure 3a) near the latitude where the tide peaks, and at 4°N (Figure 3b) near the equator where the QBO peaks. The QBO also comes into play apparently at different latitudes, and in different ways potentially.

It is well established (e.g., Lindzen and Chapman, 1970; Volland, 1988), that the diurnal tides are affected by the zonal circulation through advection. Linearized advection was invoked by Hagan et al. (1990) to relate the observed QBO and inter-annual variations of the diurnal tide. In a recent modeling study, McLandress (2002) specifically discussed the role meridional advection plays to generate the QBO signature in the diurnal tide. Considering that the QBO tends to be confined to equatorial latitudes and its signature in the relative variations of the tide are relatively large there (Figure 3), it is reasonable to believe that vertical advection could be just as important. Our analysis indeed does indicate that in Figure 4 where we present the accelerations that describe respectively the meridional and vertical advections at 18°N and 4°N . It is not clear how these accelerations specifically generate the QBO signatures, but one can

imagine that they conspire to produce the complicated patterns seen in the relative variations of the tide (Figure 3).

While the inter-annual variations in the tide are clearly related to the QBO, our model results show a great deal of variability and intermittency as well (Figures 6 and 7). The QBO signature as seen in the tide is pronounced for a few years, then virtually disappears for a few years to reappear again. We believe that this pattern of variability is a natural consequence of the fact that the QBO is only weakly tied to the seasonal cycle that dominates in the tide.

The QBO, being a non-linear auto-oscillator like the mechanical clock, can be generated in principal without any external time dependent forcing. In reality, however, the seasonal cycle acts as a pacemaker to influence the period of the QBO. The QBO thus can enhance or diminish the effect of the seasonal cycle in a particular phase, which in turn affects the seasonal and inter-annual variations of the tide.

The variability of the QBO in our model is in part generated by non-linear interactions with the Semi-annual Oscillation (Mayr et al., 1998). Our analysis shows that the QBO could be tuned, by changing for example the eddy diffusivity, to produce oscillations with periods of 18 or 30 months that are synchronized by the seasonal cycle (Mayr et al., 1998; 2001). Though less realistic, the QBO signature in the tide then would prove to be more persistent presumably.

References

- Akmaev, R. A., Simulation of large-scale dynamics in the mesosphere and lower thermosphere with the Doppler-spread parameterization of gravity waves: 2. Eddy mixing and the diurnal tide, *J. Geophys. Res.*, **106**, 1205, 2001a
- Akmaev, R. A., Simulation of large-scale dynamics in the mesosphere and lower thermosphere with the Doppler-spread parameterization of gravity waves: 1. Implementation and zonal mean climatologies, *J. Geophys. Res.*, **106**, 1193, 2001b
- Burrage, M. D., M. E. Hagan, W. R. Skinner, D. L. Wu, and P. B. Hays, Long-term variability in the solar tide observed by HRDI and simulated by the GSWN, *J. Geophys. Res.*, **19**, 2641, 1995.
- Avery, S. K., R. A. Vincent, A. Phillips, A. H. Manson, and G. R. Fraser, High latitude tidal behavior in the mesosphere and lower thermosphere, *J. Atm. Terr. Phys.*, **51**, 595, 1989

- Chan, K. L., H. G. Mayr, J. G. Mengel, and I. Harris, A stratified' spectral model for stable and convective atmospheres, *J. Comp. Phys.*, **113**, 165, 1994
- Forbes, J. M., and H. B. Garrett, Thermal excitation of atmospheric tides due to insolation absorption by O₃ and H₂O, *Geophys. Res. Lett.*, **5**, 1013, 1978
- Geller, M. A., V. A. Yudin, B. V. Khattatov, and M. E. Hagan, Modeling the diurnal tide with dissipation derived from UARS/HRDI measurements, *Ann. Geophys.*, **15**, 1198, 1997
- Hagan, M. E., M. D. Burrage, J. M. Forbes, J. Hackney, W. J. Randel, and X. Zhang, GSWM-98: Results for migrating solar tides, *J. Geophys. Res.*, **104**, 6813, 1999.
- Hagan, M. E., J. L. Chang, and S. K. Avery, Global-scale wave model estimates of non-migrating tidal effects, *J. Geophys. Res.*, **102**, 163493, 1997
- Hagan, M. E. and R. G. Roble, Modeling diurnal tidal variability with the National Center for Atmospheric Research thermosphere-ionosphere-mesosphere-electrodynamics general circulation model, *J. Geophys. Res.*, **106**, 24,869-24,882, 2001.
- Hagan, M. E., M. D. Burrage, J. M. Forbes, J. Hackney, W. J. Randel, and X. Zhang, QBO effects in the diurnal tide in the upper atmosphere, *Earth, Planets, Space*, **51**, 571, 1999
- Hays, P. B., D. L. Wu, and the HRDI science team, Observations of the diurnal tide from space, *J. Atmos. Sci.*, **51**, 3077, 1994
- Hines, C. O., Doppler-spread parameterization of gravity-wave momentum deposition in the middle atmosphere, 1, Basic formulation, *J. Atmos. Solar Terr. Phys.*, **59**, 371, 1997a
- Hines, C. O., Doppler-spread parameterization of gravity-wave momentum deposition in the middle atmosphere, 2, Broad and quasi monochromatic spectra, and implementation, *J. Atmos. Solar Terr. Phys.*, **59**, 387, 1997b
- Lieberman, R., Non-migrating diurnal tides in the equatorial middle atmosphere, *J. Atmos. Sci.*, **48**, 1112, 1991.
- Lieberman, Long-term variations of zonal mean winds and (1,1) driving in the equatorial lower thermosphere, *J. Atm. Sol. Terr. Phys.*, **59**, 1483, 1997.
- Manson, A. H., C. E. Meek, H. Teitelbaum, F. Vial, R. Schminder, D. Kuerschner, M. J. Smith, G. J. Fraser, and R. R. Clark, Climatology of semidiurnal and diurnal tides in the middle atmosphere (70-110 km) at middle latitudes (40-55°), *J. Atm. Terr. Phys.*, **51**, 579, 1989

- Mancini, E., N. A. McFarlane, and C. McLandress, Impact of the Doppler spread parameterization the simulation of the middle atmosphere circulation using the MA/ECHAM4 general circulation model, *J. Geophys. Res.*, **102**, 25,751, 1997
- Mayr H. G., J. G. Mengel, C. O. Hines, K. L. Chan, N. F. Arnold, C. A. Reddy, and N. S. Porter The Gravity Wave Doppler Spread Theory Applied in a Numerical Spectral Model of the Middle Atmosphere, Part II: Equatorial Oscillations," *J. Geophys. Res.*, **102**, 26,093, 1997.
- Mayr, H. G., J. G. Mengel, K. L. Chan, and H. S. Porter, Seasonal variations of the diurnal tide induced by gravity wave filtering, *Geophys. Res. Lett.*, **25**, 943, 1998
- Mayr H. G., J. G. Mengel, C. A. Reddy, K. L. Chan, and H. S. Porter, Variability of the Equatorial Oscillations Induced by Gravity Wave Filtering, *Geophys. Res. Lett.*, **25**, 2629, 1998.
- Mayr H. G., J. G. Mengel, C. A. Reddy, K. L. Chan, and H. S. Porter, Properties of QBO and SAO Generated by Gravity Waves, *J. Atmos. Solar-Terr. Phys.*, **62**, 1135-1154, 2000.
- Mayr, H. G., J. G. Mengel, K. L. Chan, and H. S. Porter, Mesosphere dynamics with gravity forcing: Part I, Diurnal and semidiurnal tides, *J. Atm. Solar-Terr. Phys.*, **B**, 1851, 2001
- McLandress, C., G. G. Shepherd, and B. H. Solheim, Satellite observations of thermospheric tides: Results from the Wind Imaging Interferometer on UARS, *J. Geophys. Res.*, **101**, 4093, 1996
- Mengel, J. G., Mayr, H. G., Chan, K. L., Hines, C. O., Reddy, C. A., Arnold, N. F., Porter, H. S., 1995. Equatorial oscillations in the middle atmosphere generated by small-scale gravity waves, *Geophys. Res. Lett.*, **22**, 3027
- Miyahara, S., Y. Miyoshi, and K. Yamashita, Variations of migrating and nonmigrating atmospheric tides simulated by a middle atmosphere general circulation model, *Adv. Space Res.*, **24(11)**, 1549-1558, 1999.
- Miyahara, S, Y. Toshida, and Y. Miyoshi, Dynamical coupling between the lower and upper atmosphere by tides and gravity waves, *J. Atm. Terr. Phys.*, **55**, 1039, 1993
- Strobel, D. F., Parameterization of atmospheric heating rate from 15 to 120 km due to O₂ and O₃ absorption of solar radiation, *J. Geophys. Res.*, **83**, 7963, 1978
- Talaat, E. R., and R. Lieberman, Non-migrating diurnal tides in mesospheric and lower thermospheric winds and temperatures *J. Atmos. Sci.*, **56**, 4073, 1999

- Teitelbaum, H. and F. Vial, On tidal variability induced by nonlinear interaction with planetary waves, *J. Geophys. Res.*, **96**, 14,169-14,178, 1991.
- Vincent, R. A., S. Kovalam, D. C. Fritts, and J. R. Isler, Long-term MF radar observations of solar tide in the low-latitude mesosphere: Inter-annual variability and comparison with the GSWM, *J. Geophys. Res.*, **103**, 8667, 1998.
- Vincent, R. A., T. Tsuda, and S. Kato, A comparative study of mesospheric solar tides observed at Adelaide and Kyoto, *J. Geophys. Res.*, **93**, 699, 1988.
- Walterscheid, R. L., G. G. Sivjee, G. Schubert, and R. M. Hamway, Large amplitude semidiurnal temperature variations in the polar mesopause: evidence of pseudotide, *Nature*, **324**, 1986
- Yudin, V. A., B. V. Khattatov, M. A. Geller, et al., Thermal tides and studies to tune the mechanistic tidal model using UARS observations, *Ann. Geophys.*, **15**, 1205, 1997

Figure Captions

Figure 1: Computed zonal winds, averaged over 28 days, are presented for 4°N as contour plots covering the altitude range from 10 to 100 km and the time span from 2 to 8 years. The Quasi-biennial Oscillation (QBO) with a period of about 25 months is prominent at 30 km where the winds approach 20 m/s. At higher altitudes, the Semiannual Oscillation (SAO) dominates with winds exceeding 30 m/s.

Figure 2: Computed diurnal tide at 95 km for the time span 2 to 8 years derived with a 28-day running window. Meridional (a) and zonal (b) winds are shown at 18°N . Zonal winds (c) at 4°N are shown together with a histogram. The signature of the 24-months QBO is apparent.

Figure 3: Relative variations of the zonal winds in the diurnal tide, averaged over half a year, are presented for 18°N (a) and 4°N (b). As in Figure 2, the QBO signatures are evident but are evident at all altitudes.

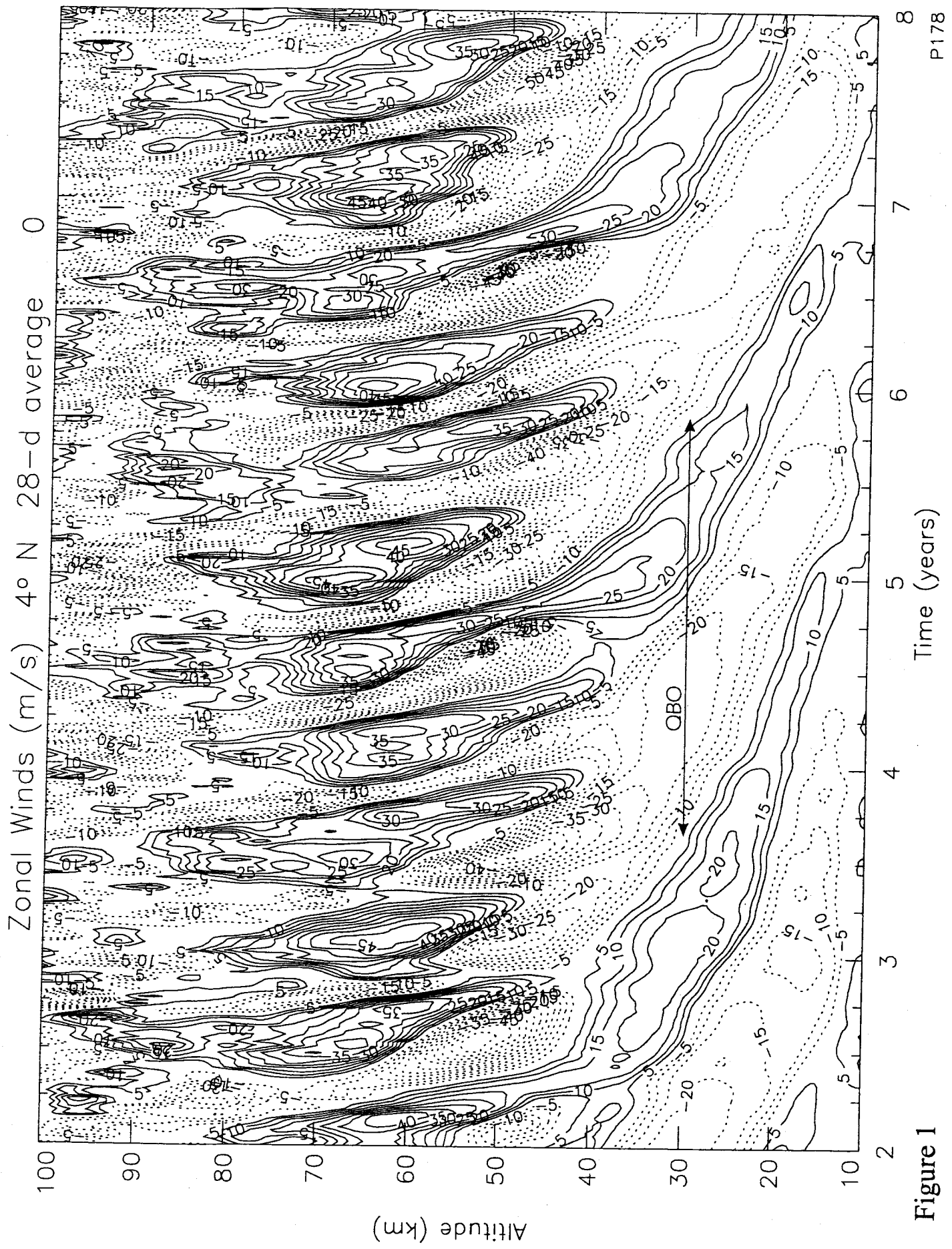
Figure 4: The linearized advection terms proportional to the tide and (a) the latitudinal gradient of the $m = 0$ zonal winds and (b) the vertical gradient of the same zonal winds are presented respectively at 18°N and 4°N . To reveal the QBO signature, the time average component is taken for the tide and the 364-day mean is applied to the zonal mean winds.

Figure 5: (a) Spectrum of zonal winds ($m = 0$) obtained from a computer run covering 26 years. For comparison, histograms for zonal and meridional winds of the diurnal tide at 4°N (b)

and 18°N (c) respectively are shown at 95 km. The spectral features describing the QBO with periods of about 24 and 28 months are also present in the tide.

Figure 6: (a) Zonal winds ($m = 0$) at 4°N , averaged over 182 days (1/2 year), are presented for a time span of 12 years to reveal the variability at altitudes above 60 km. For comparison (b), the diurnal tide is shown along with the histogram at 95 km.

Figure 7: (a) Time series of 28-day mean of zonal winds at 30 km altitude, describing the QBO at 4°N . (b) Zonal winds of diurnal tide at the same altitude and latitude obtained with a 182-day (1/2year) running window. The diurnal tide at 95 km is presented for the zonal winds at 4°N (c) and for the meridional winds at 18°N (d). Where apparent, the QBO signatures are identified.



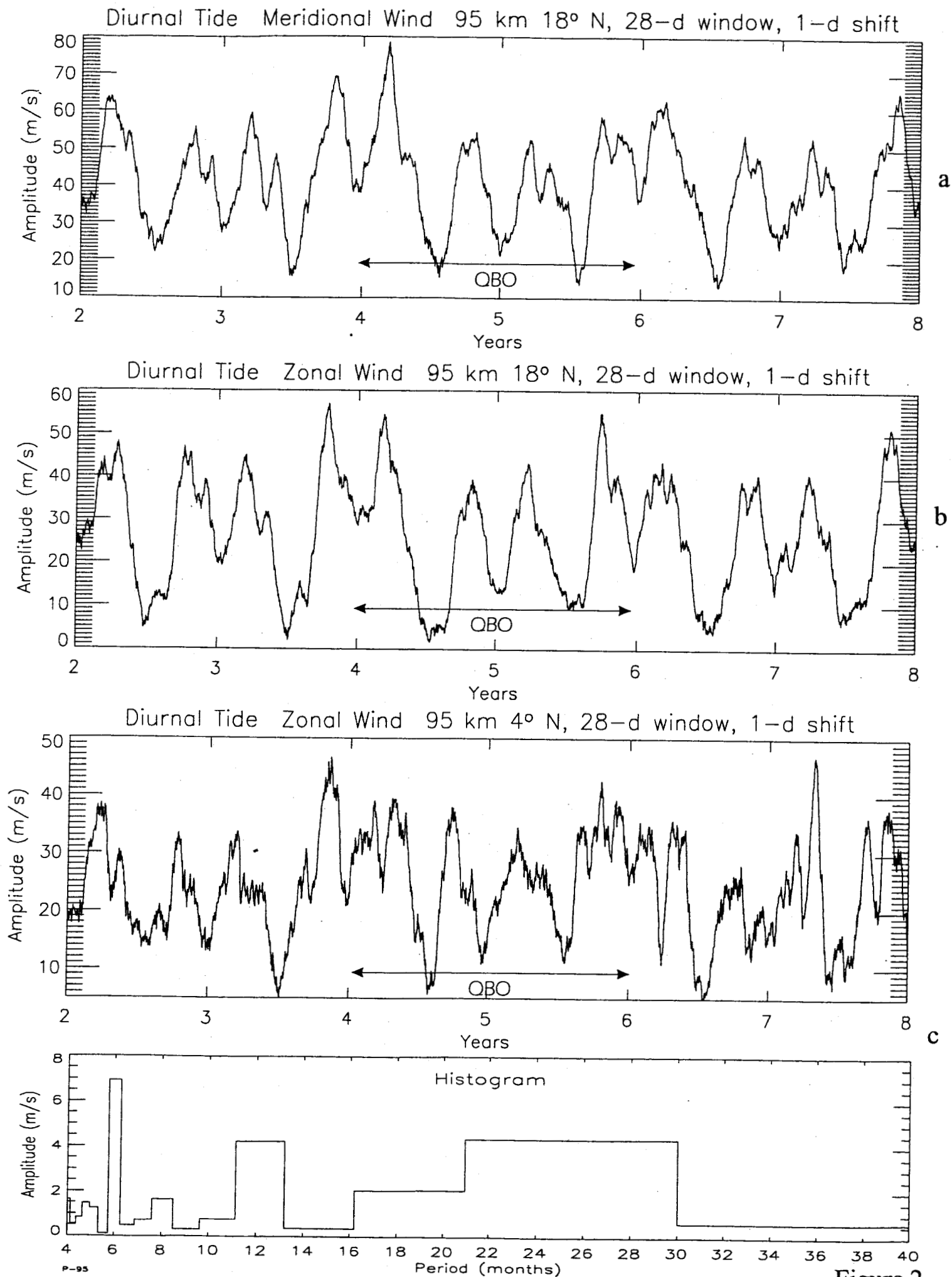
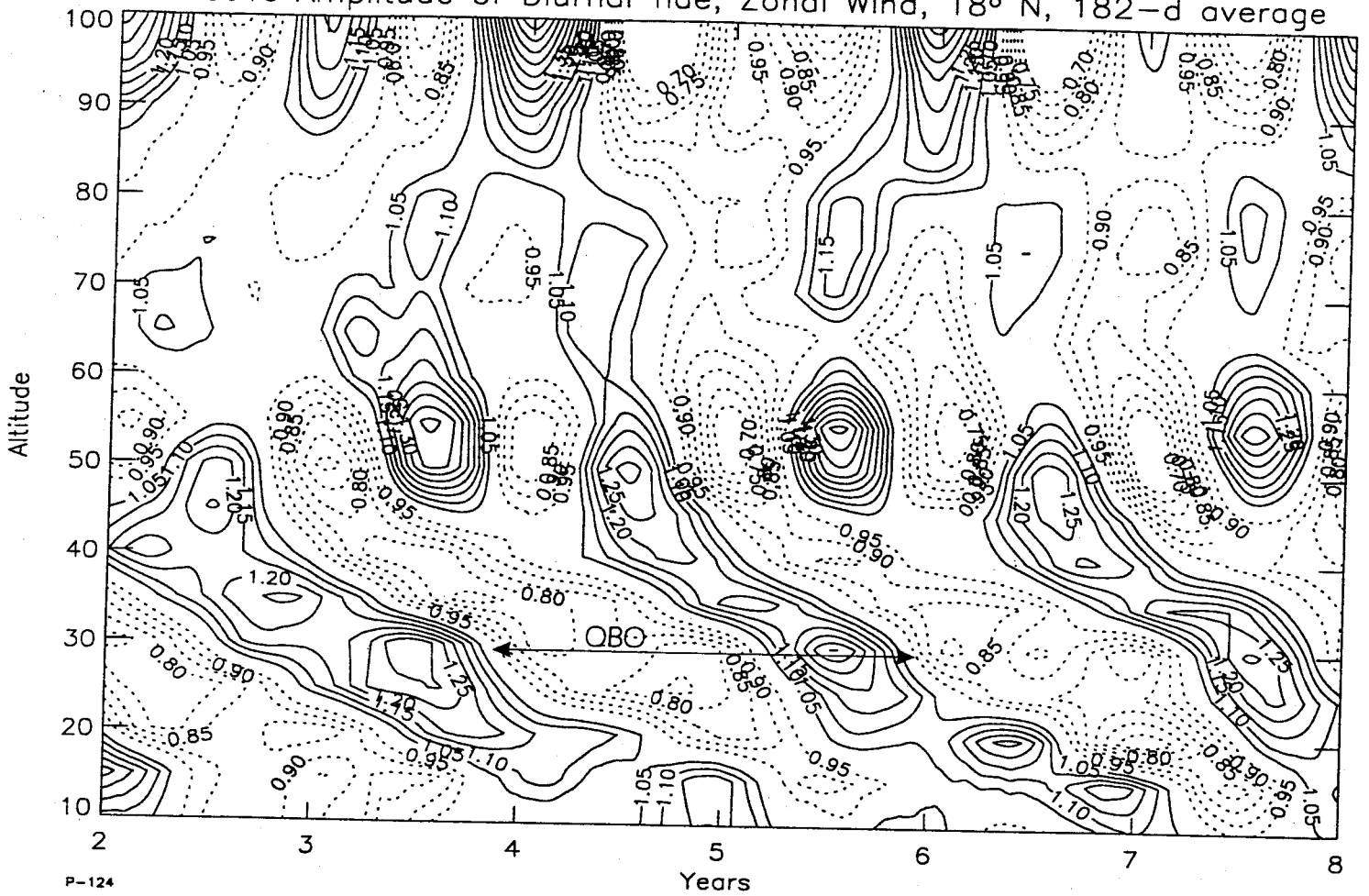


Figure 2

Relative Amplitude of Diurnal Tide, Zonal Wind, 18° N, 182-d average



Relative Amplitude of Diurnal Tide, Zonal Wind, 4° N, 182-d average

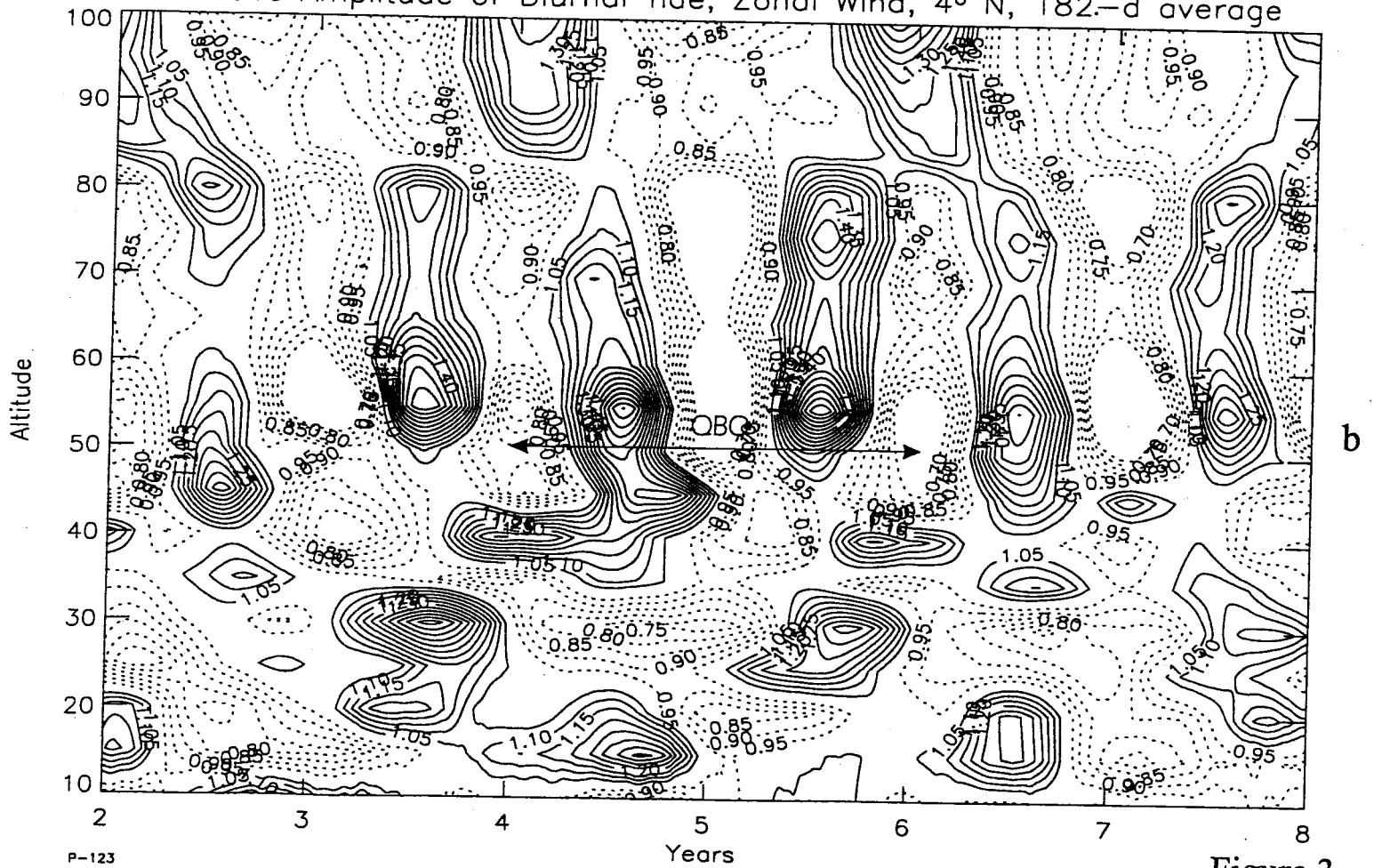


Figure 3

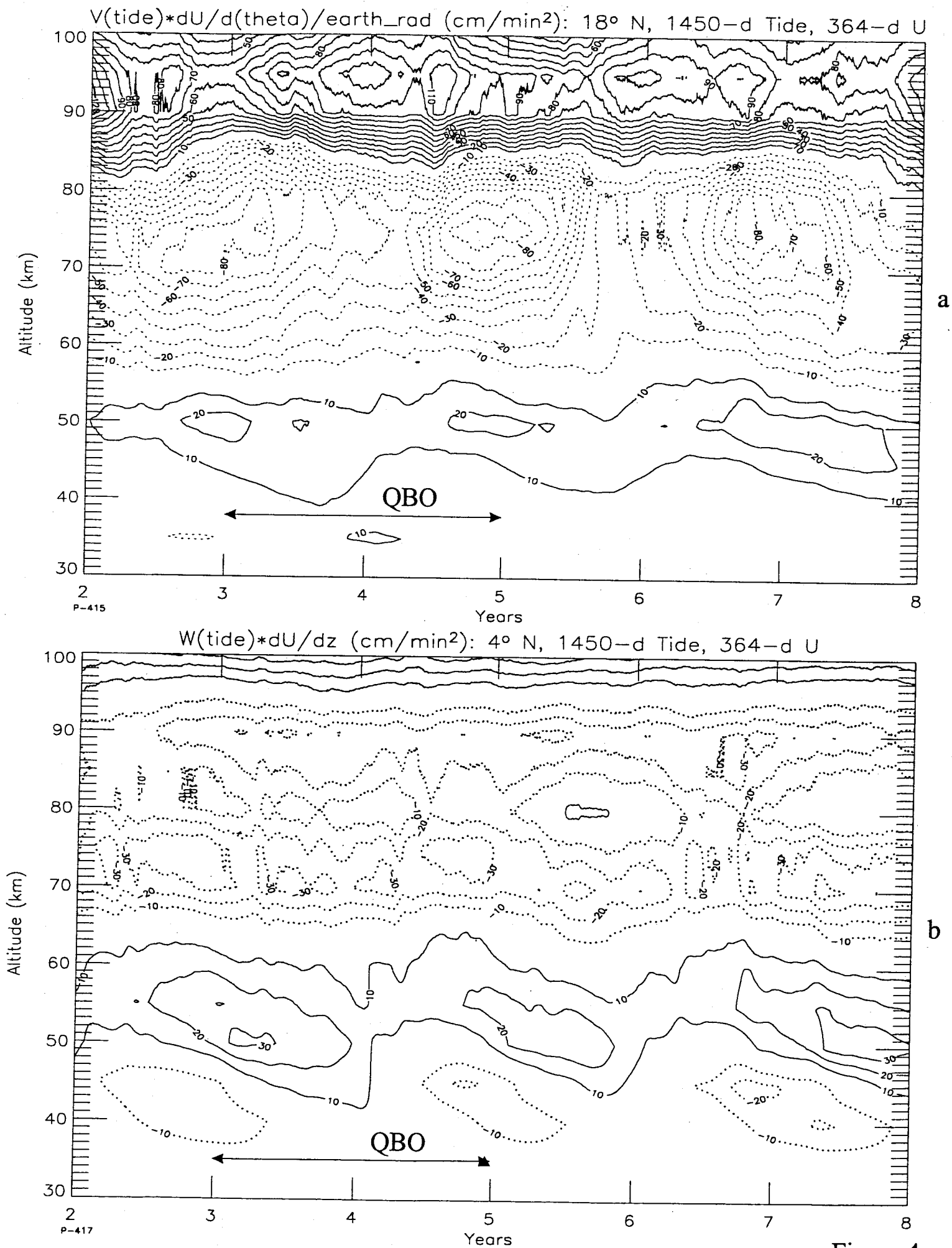


Figure 4

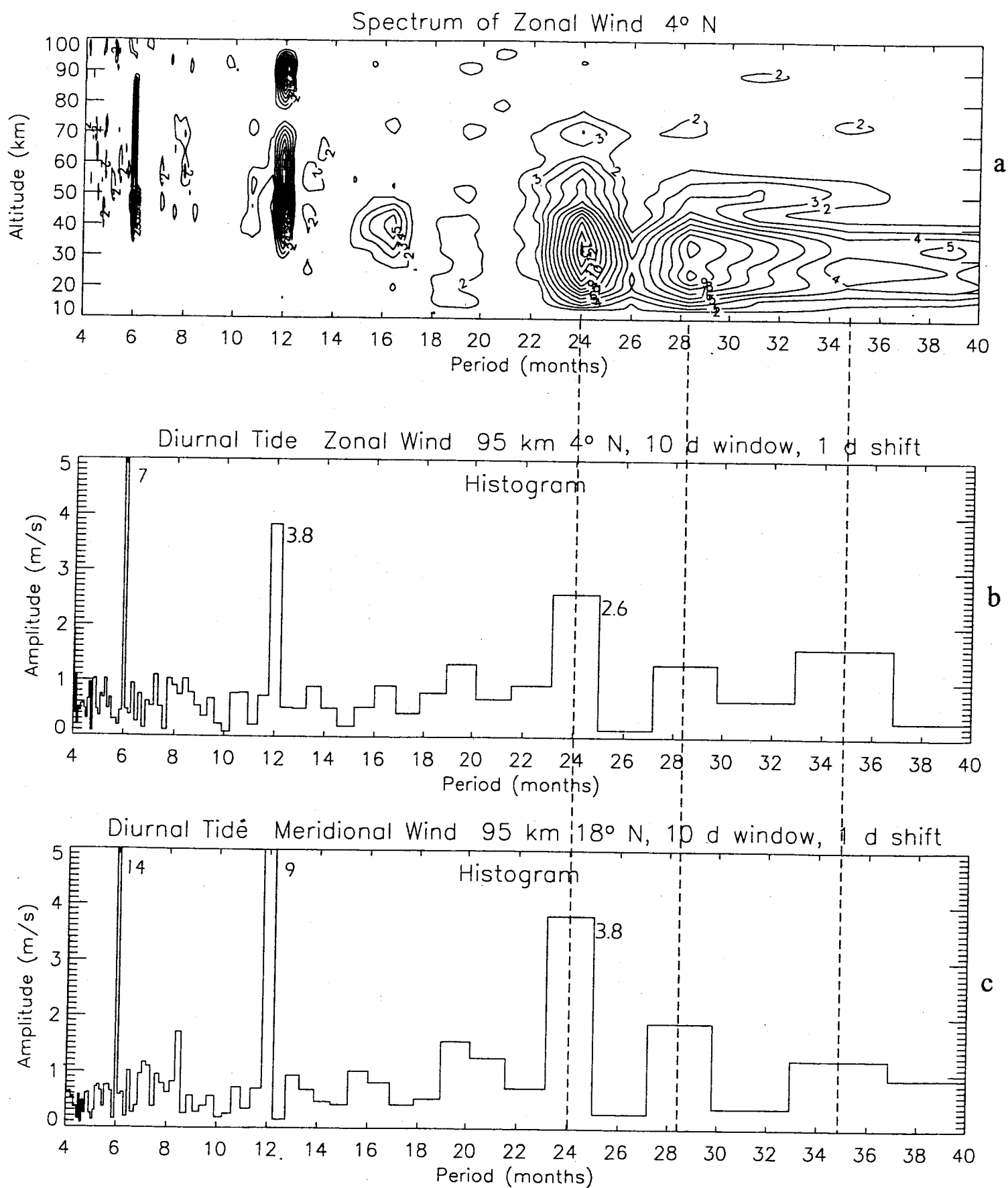
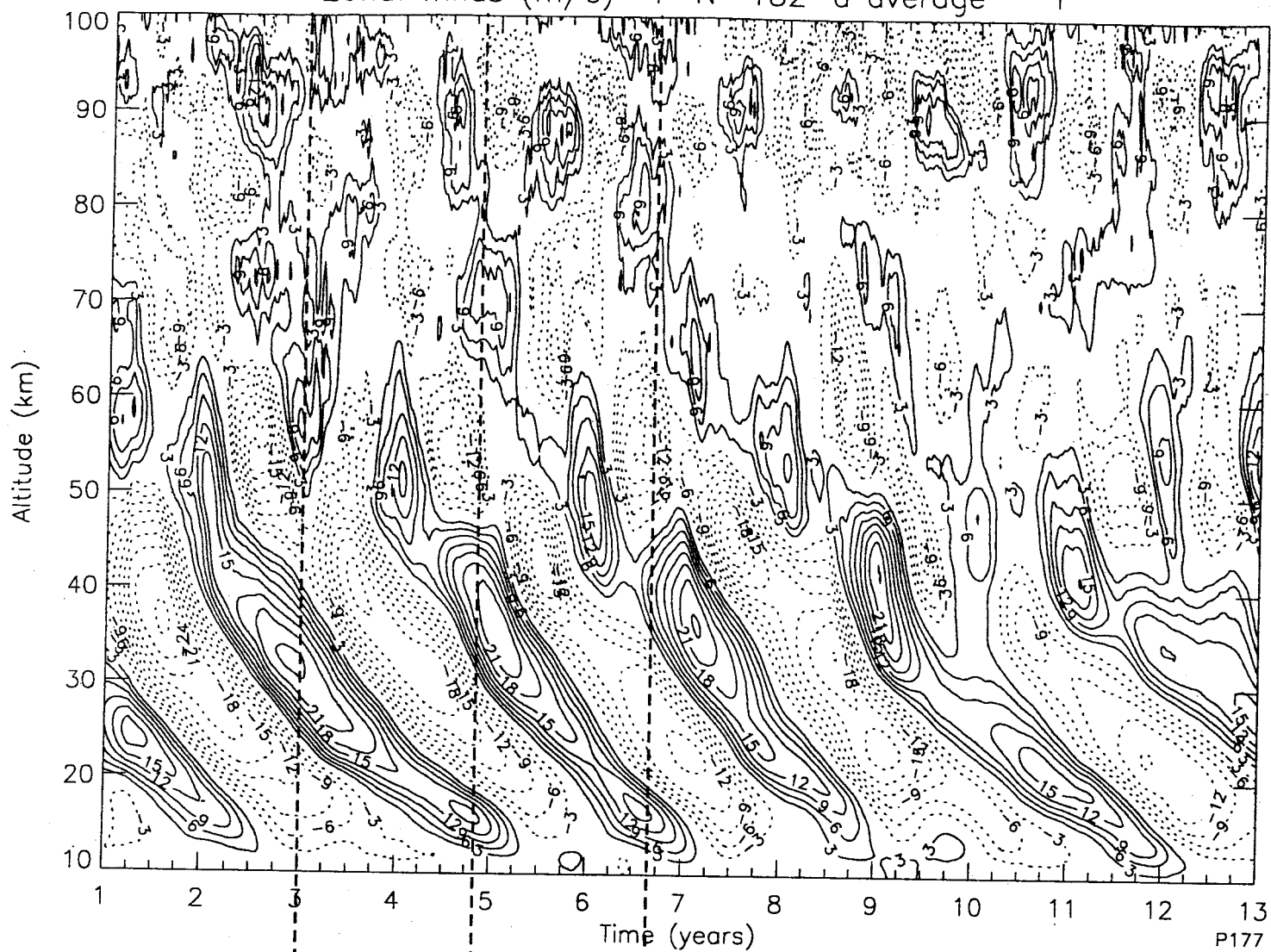


Figure 5

Zonal Winds (m/s) 4° N 182-d average 1



Diurnal tide Zonal Wind 95 km 4° N, 182-d window, 1-d shift

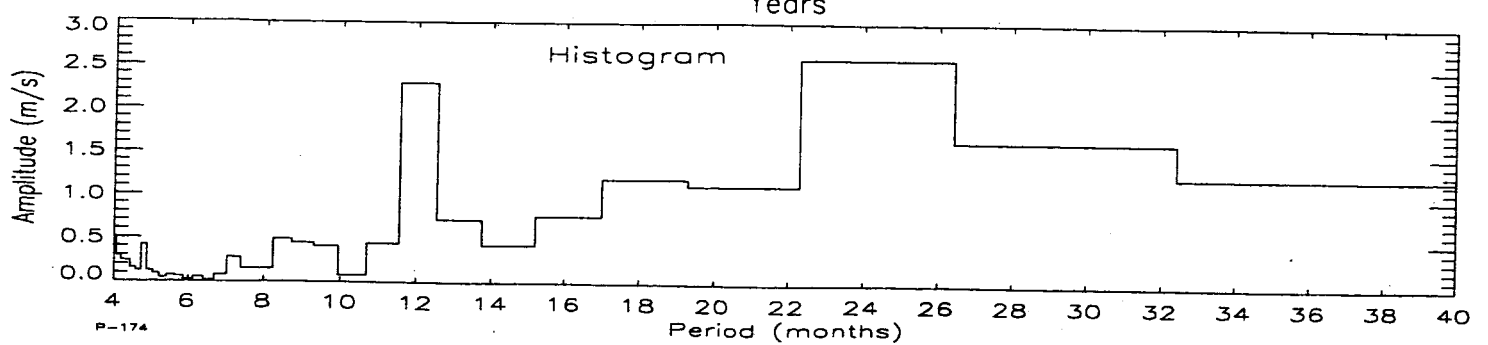
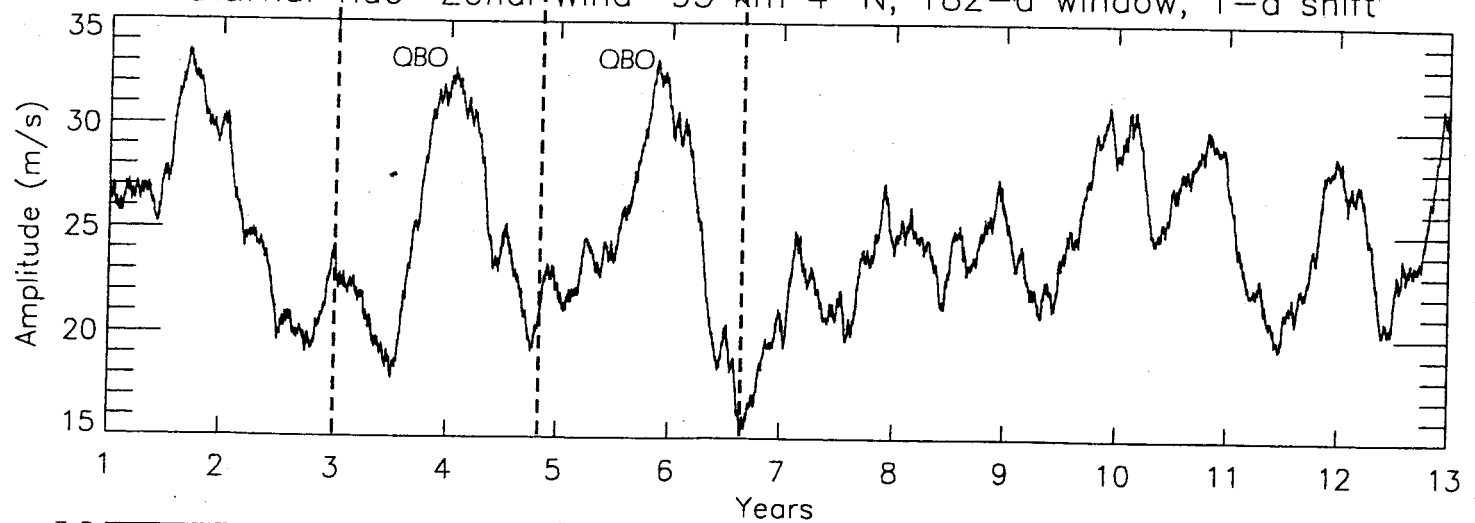


Figure 6

